Biophysical Journal, Volume *120*

Supplemental information

“Bucket brigade” using lysine residues in RNA-dependent RNA polymerase of SARS-CoV-2

Shoichi Tanimoto, Satoru G. Itoh, and Hisashi Okumura

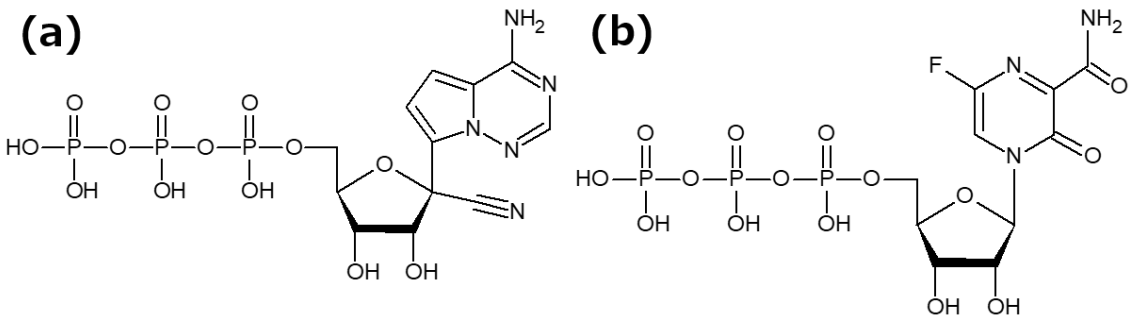

Figure S1. Chemical structures of (a) remdesivir and (b) favipiravir in the active form.

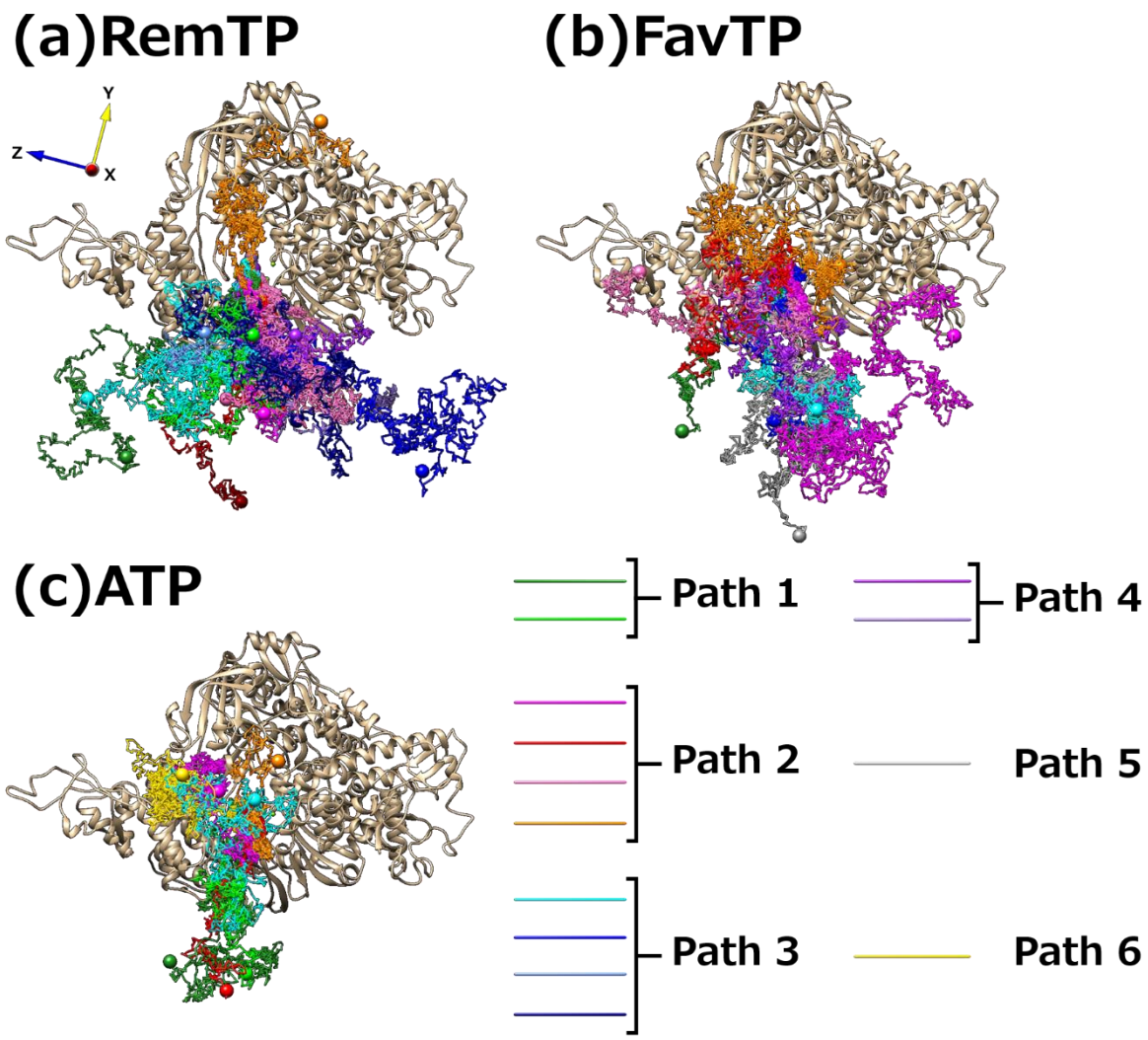

Figure S2. All trajectories of the ligands for (a) RemTP, (b) FavTP, and (c) ATP recognized by RdRp. The large spheres represent the start and end points of each trajectory. Two small light green spheres represent Mg^{2+} ions. Coordinate axes are also shown in panel (a).

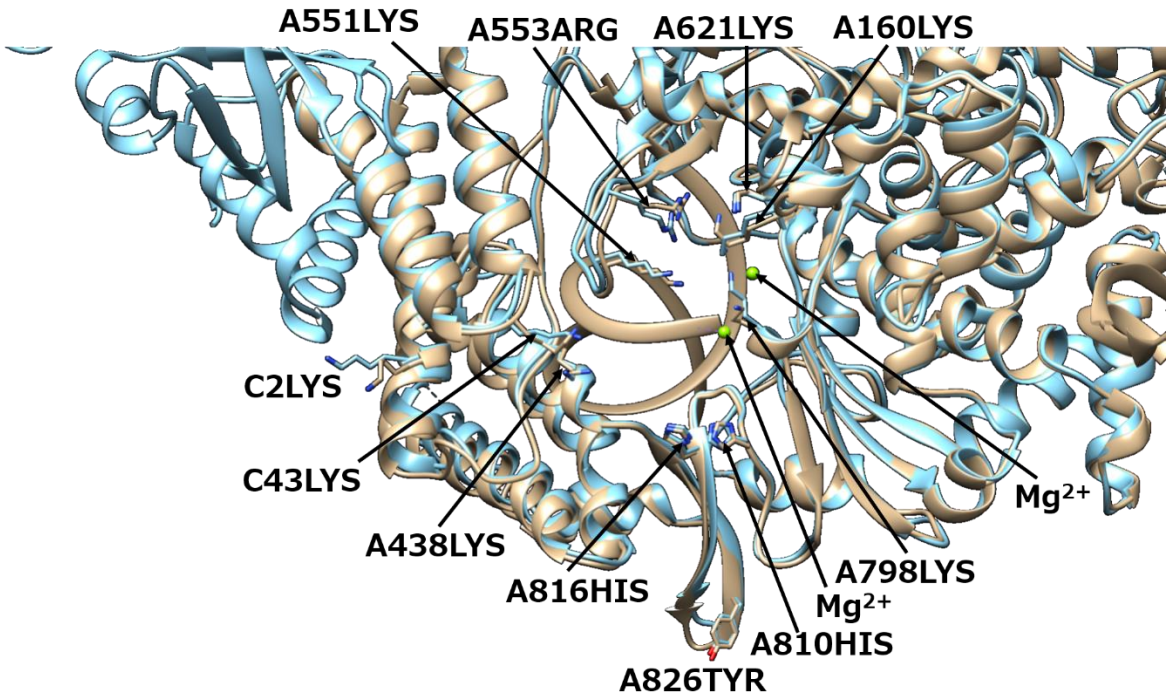

Figure S3. Superposition of the RdRp crystal structure of SARS-CoV-2 (PDB ID: 7bv2; beige) and that of SARS-CoV (PDB ID: 6nur; pale blue). The highly conserved residues that significantly contribute to the ligand recognition (A160LYS, A438LYS, A551LYS, A553ARG, A621LYS, A798LYS, A810HIS, A816HIS, A826TYR, C2LYS, and C43LYS) are represented as stick models. Two small light green spheres indicate Mg^{2+} ions. The other residues and double stranded RNA are represented as ribbon models.

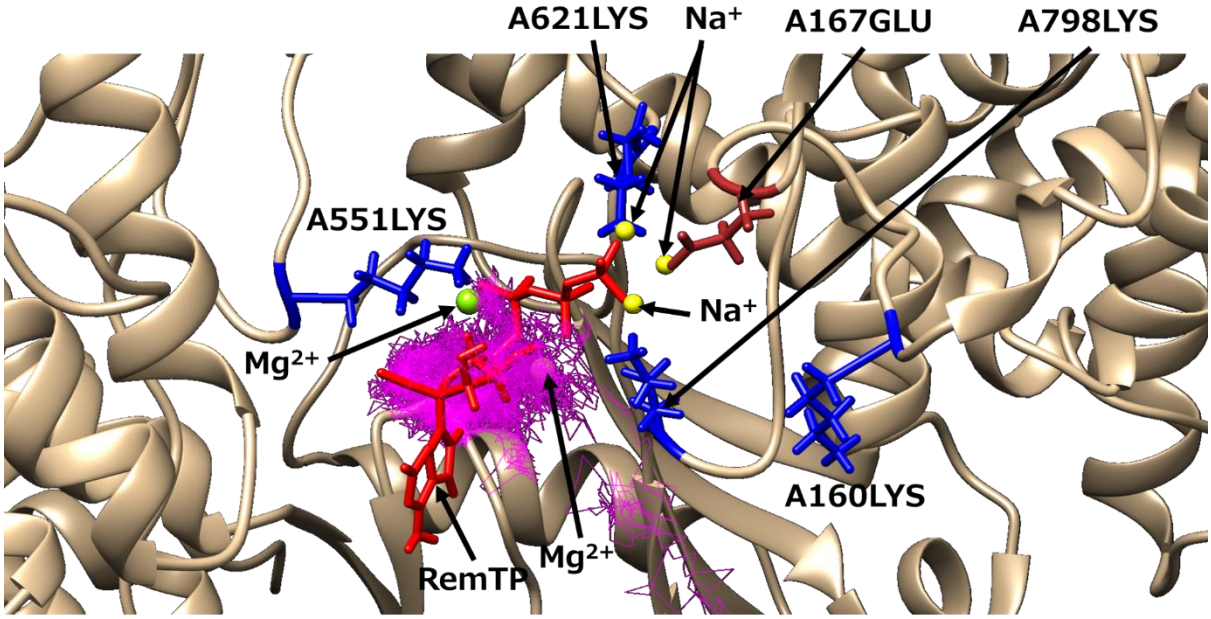

Figure S4. Characteristic structure at S4 in Fig. 5(e) with sodium ions. The representations of RemTP and residues of RdRp are the same as in Fig. 5 except for Na^{+} ions (yellow sphere).

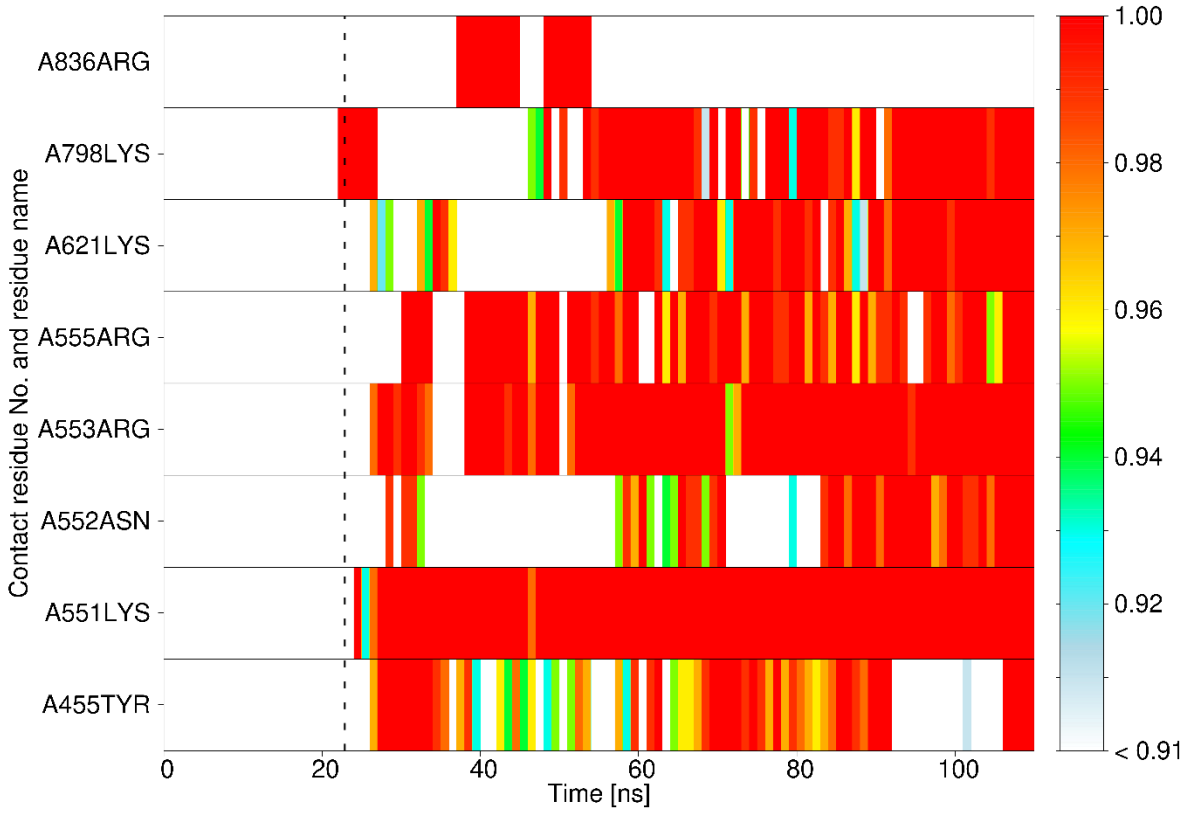

Figure S5. A representative time series of contact probabilities for each residue with RemTP in path 3. The representations are the same as in Fig. 4 in the main text.

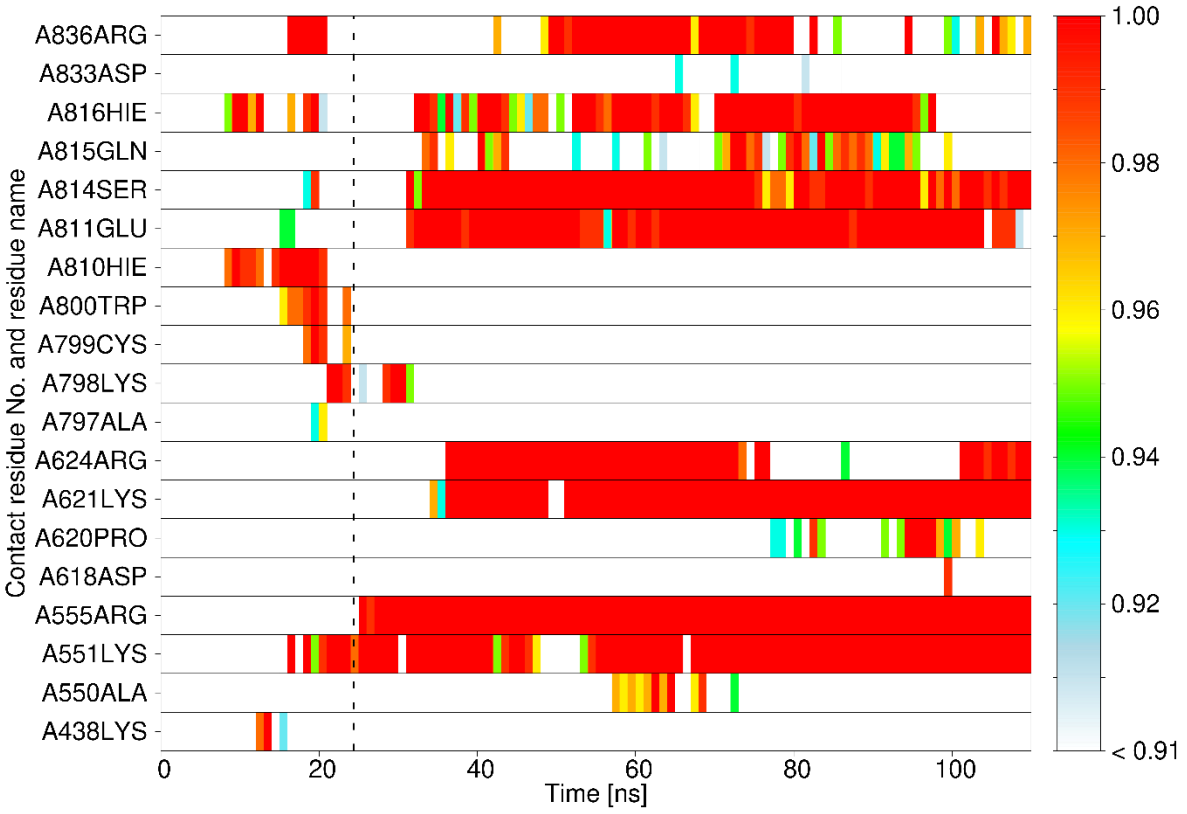

Figure S6. A representative time series of contact probabilities for each residue with RemTP in path 4. The representations are the same as in Fig. 4 in the main text.

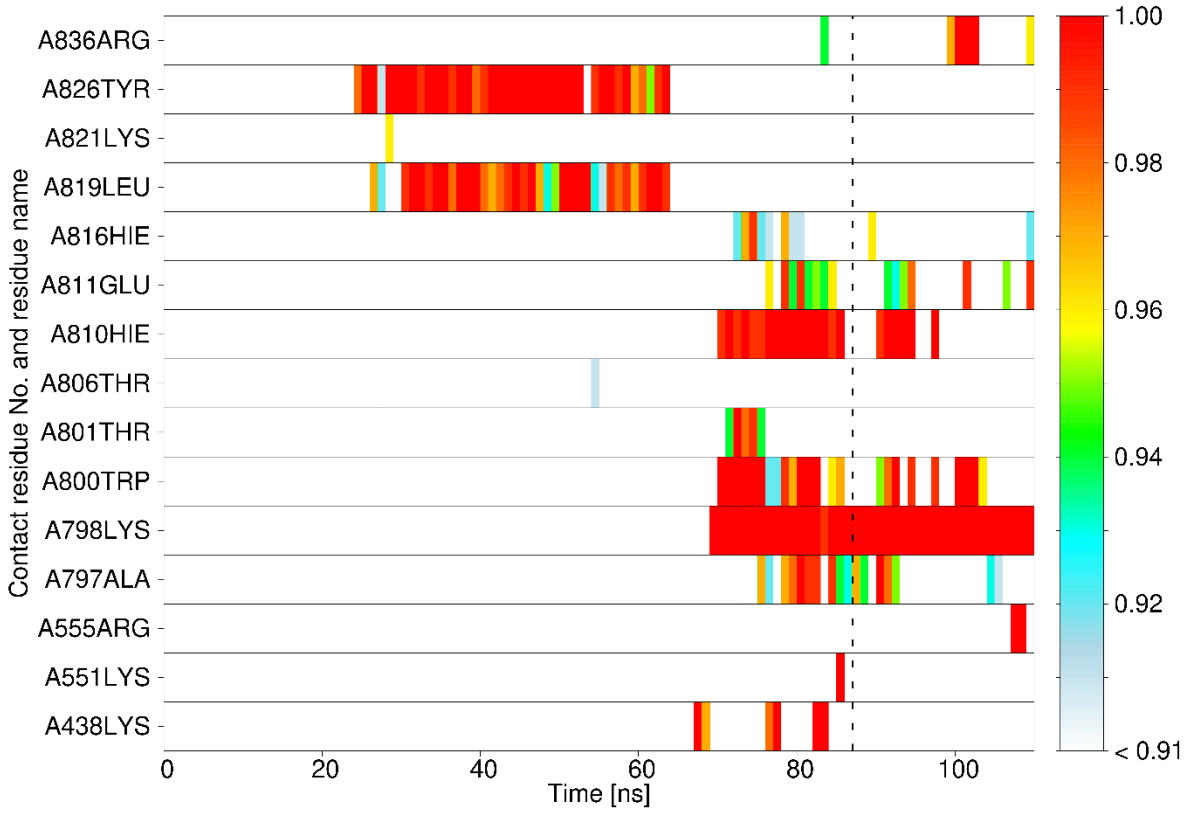

Figure S7. The time series of contact probabilities for each residue with FavTP in path 5 (a path observed only for FavTP). The representations are the same as in Fig. 4 in the main text.

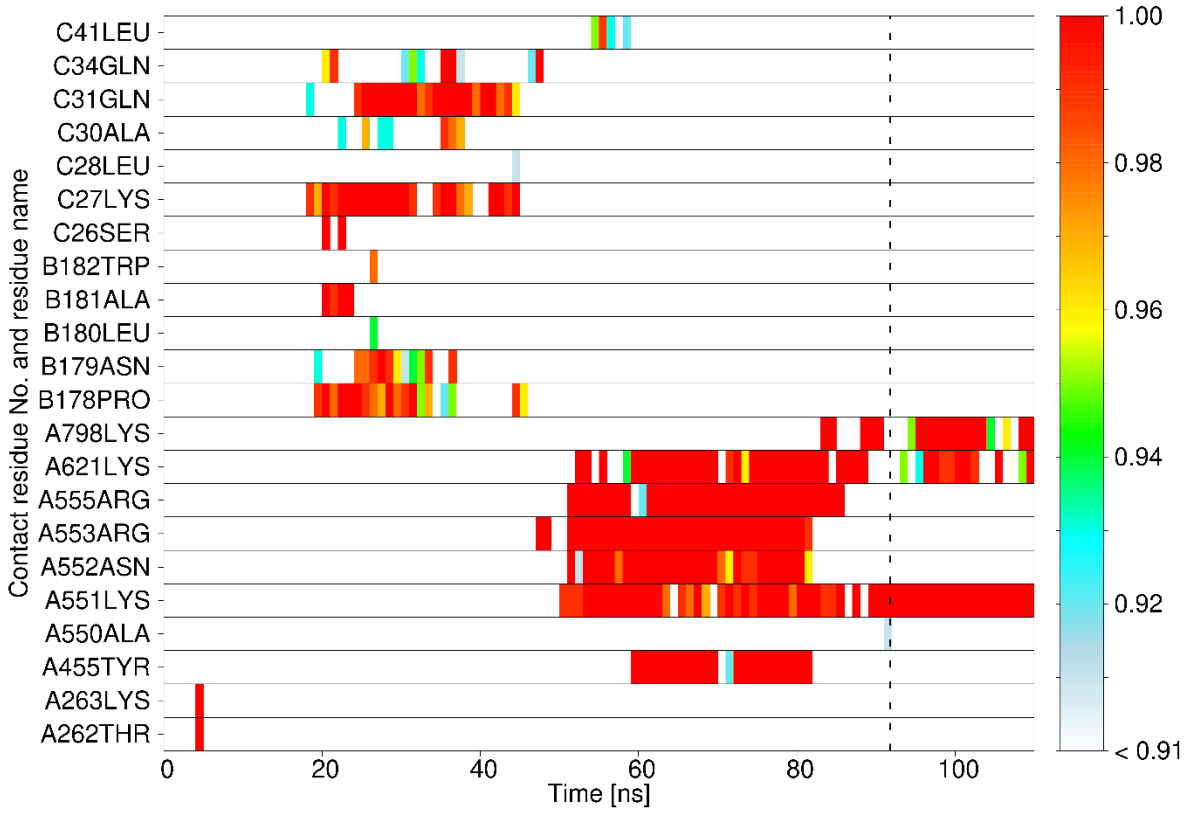

Figure S8. The time series of contact probabilities for each residue with ATP in path 6 (a path observed only for ATP). The representations are the same as in Fig. 4 in the main text.

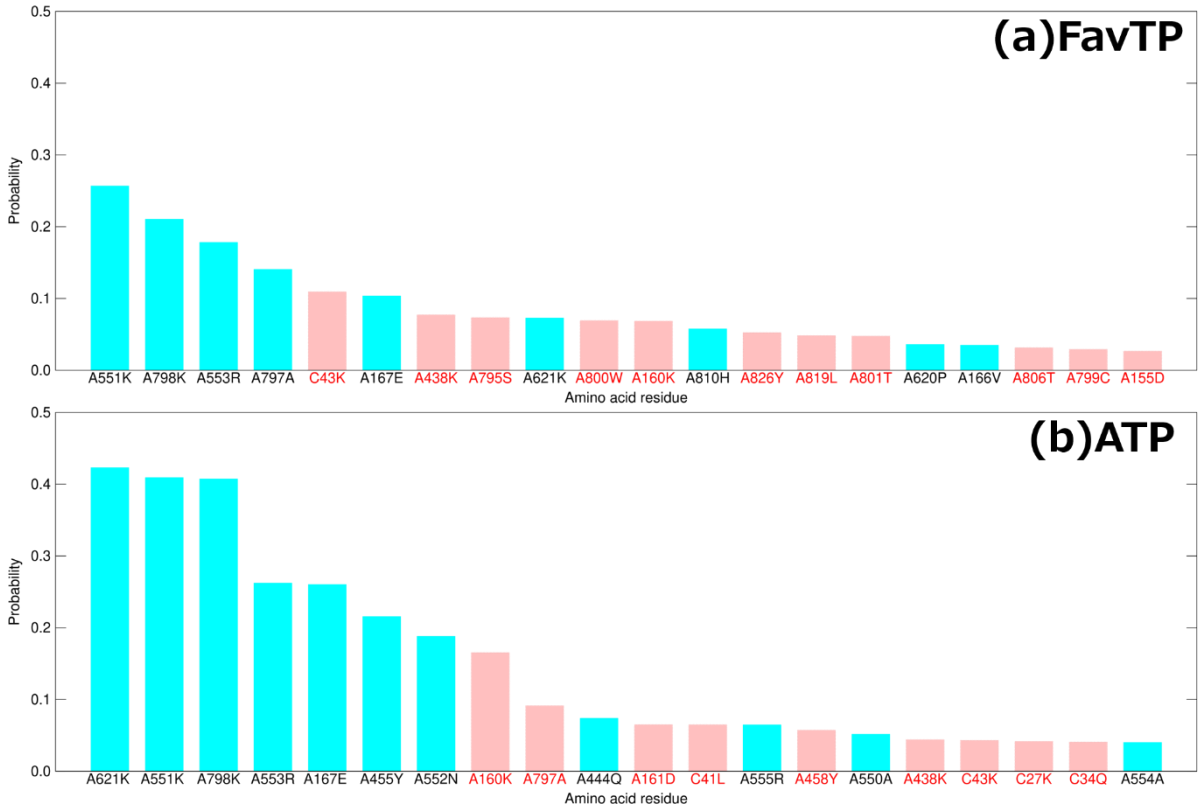

Figure S9. The average contact probabilities of the top 20 residues in contact with (a) FavTP and (b) ATP before the first contact event between Mg^{2+} ions and the ligands. Residues that are not included in the top 20 of the average contact probabilities after the first contact event (Figs. S10(b) and (c)) are shown in red letters and pink vertical bars. These contact probabilities were calculated from the trajectories with the ligand recognition events (9 trajectories for FavTP and 7 trajectories for ATP).

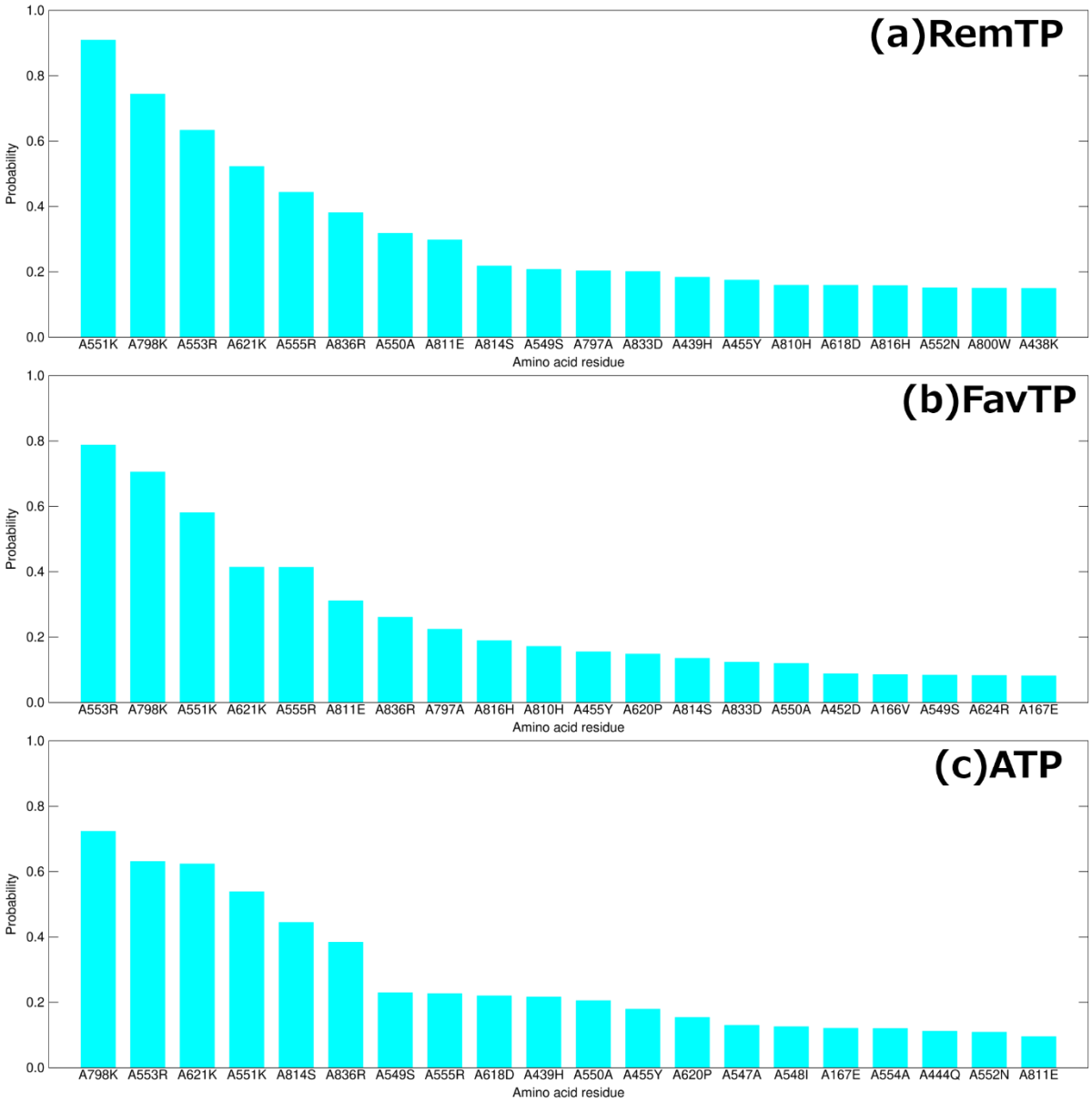

Figure S10. The average contact probabilities of the top 20 residues in contact with (a) RemTP, (b) FavTP, and (c) ATP after the first contact event between Mg^{2+} ions and the ligands. These contact probabilities were calculated from the trajectories with the ligand recognition events (12 trajectories for RemTP, 9 trajectories for FavTP, and 7 trajectories for ATP).

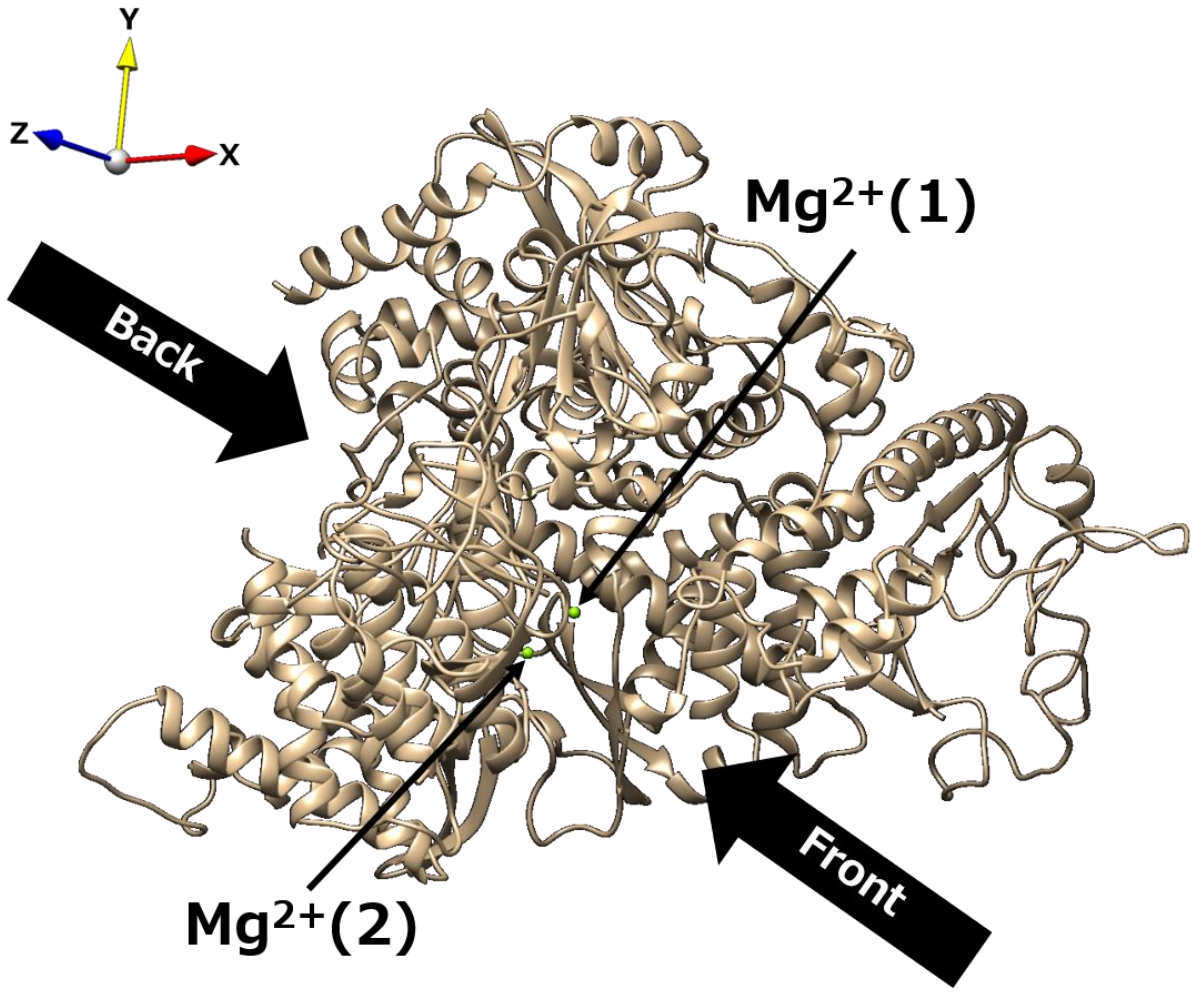

Figure S11. The definitions of the front and back sides, and the labels on two Mg^{2+} ions.

Table S1. The number of MD simulations in which ligands were recognized by RdRp from the front side (correct side) and back side (opposite side). See Fig. S11 for the definitions of the front and back sides. The definition of the ligand recognition event is the same as in Table 1 in the main text.

Ligand	Front	Back
RemTP	12	3
FavTP	9	1
ATP	7	2

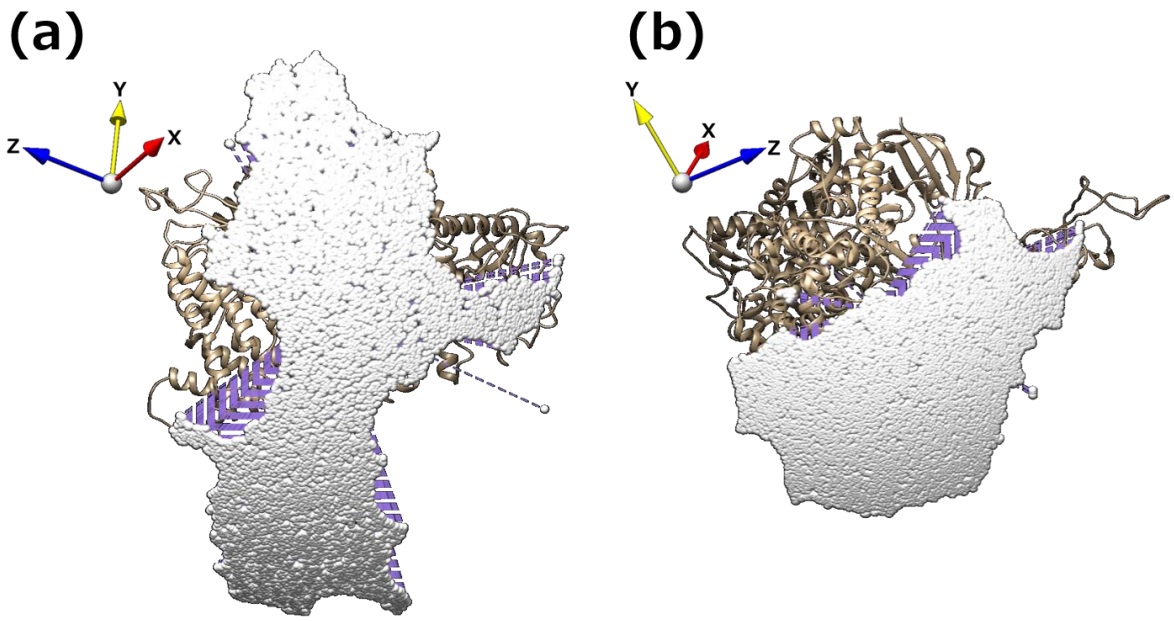

Figure S12. Parts of the spherical surface created by the solid angles with which outside is seen from Mg^{2+}(1) without being obstructed by any residues of RdRp (a) on the front side and (b) on the back side.

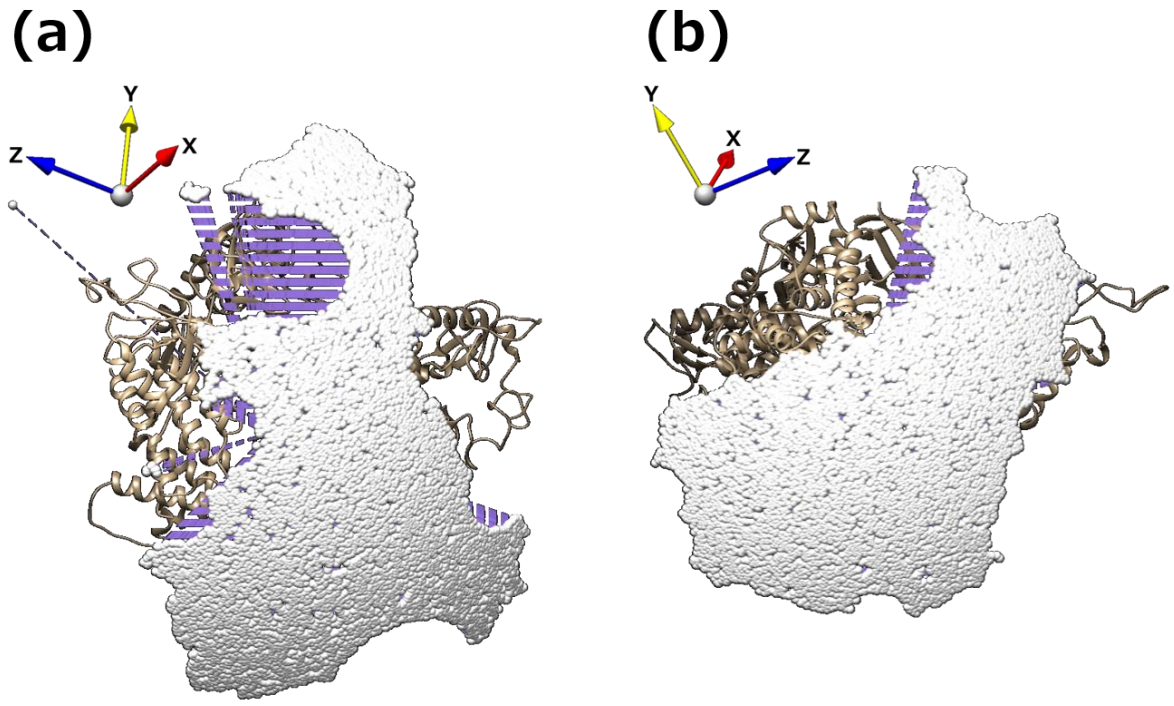

Figure S13. Parts of the spherical surface created by the solid angles with which outside is seen from Mg^{2+}(2) without being obstructed by any residues of RdRp (a) on the front side and (b) on the back side.

Video S1. Whole view of the RdRp and RemTP system.

Video S2. The RemTP recognition process in path 1.

Video S3. The FavTP recognition process in path 1.

Video S4. The ATP recognition process in path 1.

Video S5. The RemTP recognition process in path 2.

Video S6. The FavTP recognition process in path 2.

Video S7. The ATP recognition process in path 2.

Video S8. The RemTP recognition process in path 3.

Video S9. The RemTP recognition process in path 4.

Video S10. The base moiety of FavTP and the sidechain of A826TYR of RdRp formed π-π stacking in path 5.

Video S11. ATP was trapped in the gap between chain B and chain C of RdRp in path 6.